

Annular ballast resistor: Symmetry breaking, pinning, and coarsening in a globally constrained reaction-diffusion system

Baruch Meerson and Yoav Tsori

The Racah Institute of Physics, Hebrew University of Jerusalem, Jerusalem 91904, Israel

(Received 2 September 1997)

The wire ballast resistor (BR) is one of the simplest physical systems that exhibit bistability and pattern formation. An annular BR is suggested as a simple two-dimensional extension of the wire BR. The nonuniformity of the electric current density in the annular BR leads to translational symmetry breaking in the temperature domain dynamics. As a result, the steady-state position of the domain wall is “pinned” and the system exhibits coarsening. The two-phase steady-state relaxation towards it and coarsening in the annular BR are investigated analytically and numerically. [S1063-651X(98)02701-9]

PACS number(s): 82.40.Ck, 44.30.+v

I. INTRODUCTION

The wire ballast resistor (BR) represents a current-carrying iron wire put in a gas-filled cylinder, and this device has been known for a long time (see Refs. [1–5] and references therein). A closely related system is an electrically heated catalytic ribbon [6]. For a nonlinear physicist, the BR is one of the simplest and reasonably well controllable systems that exhibit pattern formation. Temperature dynamics along the wire is described by a reaction-diffusion equation with a small thermal diffusion term, the “reaction” term being the difference between the Joule heating and Newton cooling rates. Because of the characteristic S-shaped temperature dependence of the wire resistivity, the BR exhibits thermal bistability. In the constant-current regime either hot or cold domains expand until they occupy the whole wire. On the contrary, in the constant-voltage regime, domains of the two “phases” can coexist in a stable manner under the well-known “area rule” or “Maxwell construction” that sets in self-consistently owing to a global constraint imposed on the dynamics by the constant voltage [1–5,7]. The constant-voltage BR is therefore able to sustain long-lived patterns (temperature domains). However, these domains (and, more generally, domains in a globally constrained bistable reaction-diffusion equation) are to some extent degenerate, as they are only neutrally stable with respect to translations.

To the authors’ knowledge, no attempts have been made until now to extend the BR to higher dimensions. Such extensions are not straightforward, as related two- and three-dimensional scalar reaction-diffusion equations, investigated recently in other contexts [7–10], are not applicable here. Instead, one has to introduce an additional scalar field, the electric potential, that enters the thermal balance equation through the Joule heating term. The electric potential in turn is affected by the temperature field through the temperature dependence of the electric resistivity $\rho(T)$. Employing Ohm’s law and assuming that the current is quasistatic, one can reduce the problem to a set of two coupled partial differential equations: a nonlinear parabolic equation for the temperature $T(\mathbf{r}, t)$ and an elliptic equation for the potential $\phi(\mathbf{r}, t)$ that should be solved with proper initial and bound-

ary conditions (see a formulation of the problem in Sec. II). Since both equations are nonlinear and the equation for ϕ is also nonlocal, the problem is quite complicated, even in the standard limit of a slow thermal diffusion that we will adhere to throughout the paper. As a simple first step, we will consider an annular geometry and assume azimuthally symmetrical dynamics. In this case ϕ can be represented as an integral of $\rho(T)$ and most of the conveniences of a one-dimensional BR model are restored. However, the current density and therefore Joule heating are nonuniform now, as the central zone of the BR is heated more than the periphery. As we will show, this translational symmetry breaking leads to important effects that are not present in the “conventional” reaction-diffusion equation with bistability [2,4,5,7–10]. As an additional simplification, we will employ a step function for the temperature dependence of the resistivity $\rho(T)$. In this case one gets a set of *linear* equations for T in each domain, the nonlinearity entering only via the moving boundaries (“domain walls”). This simplifies the analysis considerably and enables one to investigate the annular BR dynamics analytically, even far from equilibrium. Section III addresses a two-phase steady state of the annular BR. The main result here is a unique position (pinning) of the steady-state domain wall. Because of the intrinsic nonuniformity of heating, the celebrated area rule [5] becomes irrelevant and domain wall curvature insignificant (in contrast to the conventional reaction-diffusion equation [7–10]). Section IV addresses relaxation to this two-phase steady state. Of course, the azimuthally symmetric model of the annular BR, which we employ throughout most of the paper, is meaningful only if the domain wall is stable with respect to small azimuthal perturbations. Linear stability of the azimuthally symmetric mode of the domain wall dynamics with respect to small azimuthal perturbations is indeed proved in Sec. V. Section VI shows that the annular BR exhibits coarsening: A temperature profile with two domain walls becomes simplified and only one domain wall remains. Section VII describes numerical simulations with the model and Sec. VIII summarizes the results.

II. GOVERNING EQUATIONS

Let us start with a general two-dimensional BR. Using Ohm’s law and assuming quasistationarity of the current dis-

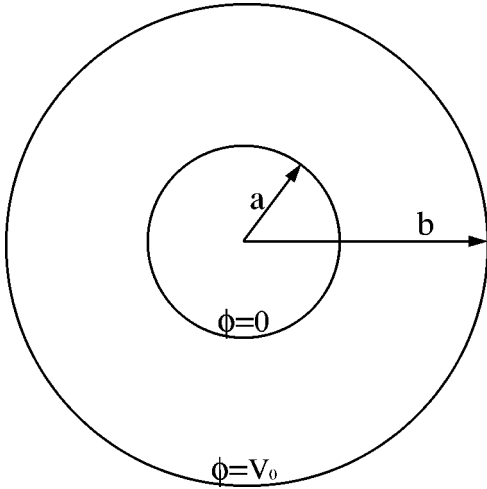


FIG. 1. Schematic of the annular ballast resistor.

tribution, we obtain the well-known elliptic equation for the electric potential:

$$\nabla \cdot \left(\frac{\nabla \phi}{\rho} \right) = 0. \quad (1)$$

This nonlocal equation is coupled, through the temperature-dependent resistivity $\rho(T)$, to the heat balance equation that accounts for the Joule heating, Newton's cooling, and thermal conduction:

$$c \frac{\partial T}{\partial t} = \frac{(\nabla \phi)^2}{\rho} - A(T - T_0) + \nabla \cdot (\kappa \nabla T), \quad (2)$$

where c is the heat capacity per unit area, κ is thermal conductivity, T_0 is a (constant) temperature of the environment, and $A = \text{const}$.

In the following, we consider a planar annular BR: a thin conducting annulus whose inner and outer circumferences have radii a and b and are kept at constant electric potentials 0 and V_0 , respectively (see Fig. 1). If we assume azimuthal symmetry, Eq. (1) yields

$$\phi(r, t) = V_0 \frac{\int_a^r \rho[T(r', t)] (r')^{-1} dr'}{\int_a^b \rho[T(r', t)] (r')^{-1} dr'}, \quad (3)$$

where r is the radial coordinate. The Joule heating term entering Eq. (2) takes the form

$$\frac{(\nabla \phi)^2}{\rho} = \frac{V_0^2 \rho[T(r, t)]}{r^2 \left[\int_a^b \rho[T(r', t)] (r')^{-1} dr' \right]^2} \quad (4)$$

and we are left with Eq. (2), a nonlinear integro-differential equation in partial derivatives. The nonlocality enters now through the integral of the temperature-dependent resistivity ρ all over the system. A further simplification is achieved when the characteristic S-type temperature dependence of the resistivity $\rho(T)$ is approximated by a step function

$$\rho(T) = \begin{cases} \rho_1 & \text{when } T < T_c \\ \rho_2 & \text{otherwise,} \end{cases} \quad (5)$$

where $\rho_2 > \rho_1$ and $T_c > T_0$. In this case the Joule heating term (4) can be calculated explicitly, separately for the two temperature intervals, and Eq. (2) decomposes into a number of *linear* partial differential equations, each for the individual domain. The matching conditions on each of the domain walls require continuity of the temperature and of its first derivative with respect to r . The simplest two-phase steady state of the BR is that with only one point $r = R(t)$, where $T(R, t) = T_c$, and this point is located far enough from the boundaries at $r = a$ and b . In this case

$$\frac{(\nabla \phi)^2}{\rho} = \begin{cases} \frac{\rho_1 V_0^2}{r^2 [\rho_2 \ln(R/a) + \rho_1 \ln(b/R)]^2}, & a < r < R(t) \\ \frac{\rho_1 V_0^2}{r^2 [\rho_2 \ln(R/a) + \rho_1 \ln(R/b)]^2}, & R(t) < r < b. \end{cases} \quad (6)$$

Therefore, we obtain two equations, one for the central ("hot") zone, the other for the peripheral ("cold") zone. Rewriting these equations in a dimensionless form, we get

$$T_t = T_{rr} + \frac{1}{r} T_r - T + \frac{a^2 P_2^2}{r^2 [\ln(R/a) + \varepsilon \ln(b/R)]^2}, \quad a < r < R(t) \quad (7a)$$

$$T_t = T_{rr} + \frac{1}{r} T_r - T + \frac{a^2 P_1^2}{r^2 [\ln(R/a) + \varepsilon \ln(b/R)]^2}, \quad R(t) < r < b, \quad (7b)$$

where indices t and r mean the corresponding derivatives. We have set $\kappa = \text{const}$; introduced the following scaled variables: radius $\hat{r} = r/\delta_w$, time $\hat{t} = At/c$, and temperature $\hat{T} = (T - T_0)/(T_c - T_0)$ and the following scaled parameters: $\varepsilon = \rho_1/\rho_2$, $P_1 = P_2 \sqrt{\varepsilon}$, $\delta_w = (\kappa/A)^{1/2}$, and

$$P_2 = \frac{V_0}{a [\kappa \rho_2 (T_c - T_0)]^{1/2}}; \quad (8)$$

and omitted the carets. The inner and outer radii a and b of the annular BR and the domain wall position R are normalized accordingly. For concreteness, let the inner and outer circumferences be kept at constant temperatures. In the scaled units, $T(r = a, t) = T_{\text{in}} > 1$ and $T(r = b, t) = T_{\text{out}} < 1$. The matching conditions require continuity of T and T_r at $r = R$ with $T(r = R, t) = 1$.

III. TWO-PHASE STEADY STATE

A two-phase steady-state solution of Eqs. (7) (depicted in Fig. 2) corresponds to a hot central domain and cold peripheral domain being in equilibrium, with a fixed domain wall position $R = R_*$. In general, there are two boundary layers close to the boundaries $r = a$ and $r = b$. Because of linearity,

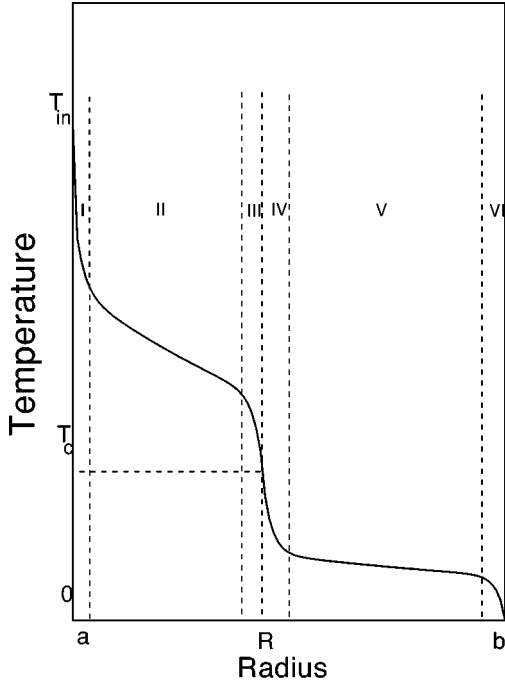


FIG. 2. Annular BR with a single azimuthally symmetric domain wall. Regions I and VI are the inner and outer boundary layers, and regions II and V correspond to the large-scale temperature profiles, regions III and IV are the inner and outer parts of the domain wall.

Eqs. (7) with $T_t=0$ can be solved exactly in terms of the Bessel functions. Instead, we will obtain a simpler approximate solution by the matched asymptotic expansion [11] based on the assumption that the characteristic domain wall width δ_w (which is of order unity in the scaled variables) is much less than the “size of the system” L , by which we will usually mean the domain size.

It can be checked that the terms including T_r can always be neglected (in contrast to the conventional globally constrained reaction-diffusion equation with bistability, where the curvature correction proves to be important [7–10]). Far from the domain wall and from the boundaries one can also neglect the T_{rr} terms. The resulting “large-scale” steady-state solution T_{LS} is

$$T_{LS}^< = \frac{a^2 P_2^2}{r^2 [\ln(R/a) + \varepsilon \ln(b/R)]^2} \quad (9)$$

for the central domain and

$$T_{LS}^> = \frac{a^2 P_1^2}{r^2 [\ln(R/a) + \varepsilon \ln(b/R)]^2} \quad (10)$$

for the peripheral domain. In the dimensional variables the temperature profiles (9) and (10) are independent of the value of thermal diffusivity κ . They develop during the rapid first stage of the dynamics, whose duration is of order c/A (see Sec. IV).

Now consider the hot part of the domain wall. Mathematically, we assume that $R-r \ll R$ and replace r by R in the denominator of the Joule heating term. Equation (7a) becomes

$$T_{rr} - T + \frac{a^2 P_2^2}{R^2 [\ln(R/a) + \varepsilon \ln(b/R)]^2} = 0. \quad (11)$$

This equation is immediately solved and the solution has two arbitrary constants. We set one of them equal to zero in order to match the solution with the large-scale solution (9) and eliminate the divergence at large negative $r-R$. The second constant is found from the condition $T(r=R) = 1$. The result is

$$T_{DW}^< = \left(1 - \frac{a^2 P_2^2}{R^2 [\ln(R/a) + \varepsilon \ln(b/R)]^2} \right) e^{r-R} + \frac{a^2 P_2^2}{R^2 [\ln(R/a) + \varepsilon \ln(b/R)]^2}. \quad (12)$$

Similarly, we solve the equation for the steady-state boundary layer near $r=a$. Here we replace r by a in the heating term of Eq. (7a), solve the resulting equation, and find two arbitrary constants by matching the solution with the large-scale solution (9) and using the boundary condition $T(r=a) = T_{in}$. The result is

$$T_{BL}^< = \left(T_{in} - \frac{a^2 P_2^2}{R^2 [\ln(R/a) + \varepsilon \ln(b/R)]^2} \right) e^{a-r} + \frac{P_2^2}{[\ln(R/a) + \varepsilon \ln(b/R)]^2}. \quad (13)$$

The composite approximation [11] makes it possible to comprise the three (overlapping) asymptotics (9), (12), and (13) in a single approximation, valid for the whole central domain $a \leq r \leq R$:

$$T_{r < R} = \left(T_{in} - \frac{P_2^2}{[\ln(R/a) + \varepsilon \ln(b/R)]^2} \right) e^{a-r} + \left(1 - \frac{a^2 P_2^2}{R^2 [\ln(R/a) + \varepsilon \ln(b/R)]^2} \right) e^{r-R} + \frac{a^2 P_2^2}{r^2 [\ln(R/a) + \varepsilon \ln(b/R)]^2}. \quad (14)$$

The same procedure for the peripheral domain $R \leq r \leq b$ yields the composite approximation

$$\begin{aligned}
T_{r>R} = & \left(T_{\text{out}} - \frac{a^2 P_1^2}{b^2 [\ln(R/a) + \varepsilon \ln(b/R)]^2} \right) e^{r-b} \\
& + \left(1 - \frac{a^2 P_1^2}{R^2 [\ln(R/a) + \varepsilon \ln(b/R)]^2} \right) e^{R-r} \\
& + \frac{a^2 P_1^2}{r^2 [\ln(R/a) + \varepsilon \ln(b/R)]^2}. \quad (15)
\end{aligned}$$

The first term corresponds to the boundary layer near $r=b$, the second one to the cold part of the domain wall, and the third to the large-scale solution. The expressions for $T_{r>R}$ and $T_{r<R}$ satisfy the continuity of the temperature at $r=R$.

Now we use the continuity of T_r and find the equilibrium position of the domain wall $R=R_*$. The main contribution to the derivative T_r in this region is from the domain wall terms. Therefore, differentiating Eqs. (14) and (15) with respect to r and equating them at $r=R_*$, we arrive at the algebraic equation

$$R_* \left(\ln \frac{R_*}{a} + \varepsilon \ln \frac{b}{R_*} \right) = a P_2 \left(\frac{1+\varepsilon}{2} \right)^{1/2}. \quad (16)$$

The left-hand side of Eq. (16) is a monotonically increasing function of R_* ; therefore, if a solution with $a < R_* < b$ exists, it is single. One can check that such a solution exists if the scaled voltage P_2 obeys the double inequality

$$\left(\frac{2\varepsilon^2}{1+\varepsilon} \right)^{1/2} \frac{b}{\ln \frac{b}{a}} \leq P_2 \leq \left(\frac{2}{1+\varepsilon} \right)^{1/2} \frac{b}{a} \ln \frac{b}{a}. \quad (17)$$

For P_2 outside the interval specified by the double inequality (17), R_* formally goes beyond the system boundaries, which means nonexistence of a two-phase steady state. The region of the plane of the control parameters (ε, P_2) where a two-phase steady state exists is shown in Fig. 3. Equation (16) implies that, in contrast to the wire BR, the steady-state domain wall is ‘‘pinned’’: The wall position depends solely on the system parameters (scaled voltage, resistivity ratio, and geometric dimensions) and is independent, within broad limits, of the initial temperature profile.

Equations (14) and (15), with R_* found from Eq. (16), imply coexistence of the hot and cold domains only if each of the equations describes a monotonically decreasing function of r . These conditions can be represented as a double inequality, imposed on R_* :

$$P_2 \varepsilon^{1/2} < \frac{R_*}{a} \left(\ln \frac{R_*}{a} + \varepsilon \ln \frac{b}{R_*} \right) < P_2. \quad (18)$$

Now let us briefly discuss two limiting cases: $\varepsilon=1$ and $\varepsilon=0$. The first limit is not very interesting, as it corresponds to a temperature-independent resistivity (and hence no bistability). One must expect here a single one-phase domain all over the system (with boundary layers at the ends). It is easy to check that the composite approximations (14) and (15) indeed yield this result, as the domain wall terms vanish in both equations, while the large-scale terms become identical. Also, Eq. (16) predicts $R_* = a P_2 / \ln(b/a)$ in this case: a natu-

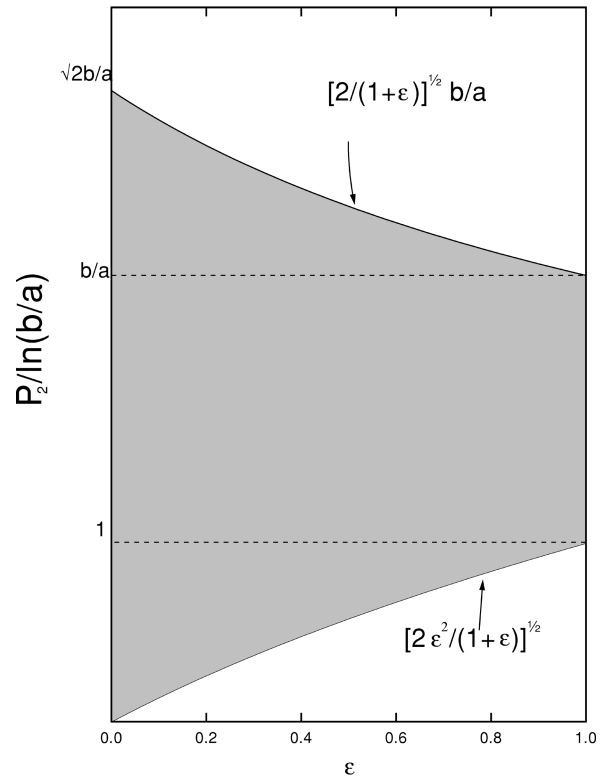


FIG. 3. Region of existence of the two-phase steady state (shown in gray) in the plane of control parameters ε and P_2 .

ral result following from the large-scale solution. We will assume in the following that ε is not too close to unity.

The second limit $\varepsilon=0$ is much more meaningful, as it simulates a transition from a normal metal to superconductor [2]. In the annular BR, the normal phase will be represented by the central domain and superconducting phase by the peripheral domain. For $\varepsilon=0$, Eq. (16) for the domain wall location can be rewritten as

$$\frac{R_*}{a} \ln \frac{R_*}{a} = \frac{P_2}{\sqrt{2}}. \quad (19)$$

The left inequality in Eq. (17) is satisfied automatically now, while the right one takes the form

$$P_2 \leq \sqrt{2} \frac{b}{a} \ln \frac{b}{a}. \quad (20)$$

Also, in view of Eq. (19), the double inequality (18) is satisfied automatically in this case.

IV. RELAXATION TO STEADY STATE

Now let us turn to relaxation of a single domain wall towards the two-phase steady state. As we will check later, our basic inequality $\delta_w \ll L$ (in the physical units) means that there are two different time scales in the dynamics and the relaxation consists of two stages, similar to the conventional reaction-diffusion equation, exhibiting bistability [4,5,7]. The cooling (heating) time scale c/A is ‘‘fast.’’ During the fast first stage, the annular BR develops hot and cold regions, corresponding to the initial condition, and a domain wall

between them. By the end of the fast stage, the large-scale parts of the temperature profiles of each of the domains are described by the steady-state results (9) and (10), but with a time-dependent $R(t)$. We are mainly interested in the subsequent, much slower, diffusion stage [with a time scale of order $Lc/(\kappa A)^{1/2}$; see later], when $R(t)$ approaches its steady-state value R_* , and the temperature profile adjusts accordingly. The moving domain wall can be described by a traveling-wave solution with a slowly varying speed $v(t)$: $T(r,t) = \Theta(\xi)$, where $\xi = r - \int^t v(t') dt'$. The speed is related to the domain wall position: $\dot{R}(t) = v$. Let us start with the hot part of the moving domain wall. After substitution, Eq. (7a) reads

$$\Theta_{\xi\xi} + v\Theta_{\xi} - \Theta + \frac{a^2 P_2^2}{r^2 [\ln(R/a) + \varepsilon \ln(b/R)]^2} = 0. \quad (21)$$

Treating the slowly varying $v(t)$ and $R(t)$ as constant, we can easily solve this linear equation. In much the same way as for the two-phase steady state, the domain wall solution has to match the large-scale solution. Therefore, one of the two arbitrary constants vanishes, while the other is determined by the condition $\Theta(\xi=0) = 1$. Returning to the original variables r and t and setting $r \approx R(t)$, we arrive at the following temperature profile for the hot part of the domain wall:

$$T_{\text{DW}}^< = \left(1 - \frac{a^2 P_2^2}{R^2 [\ln(R/a) + \varepsilon \ln(b/R)]^2} \right) e^{\mu^+(r-R)} + \frac{a^2 P_2^2}{R^2 [\ln(R/a) + \varepsilon \ln(b/R)]^2}, \quad (22)$$

where

$$\mu^{\pm} = \frac{-v \pm \sqrt{v^2 + 4}}{2}.$$

For the hot-side boundary layer we obtain the same result as in Sec. III, but with a time-dependent $R(t)$ instead of R_* . Finally, we can write the following composite approximation for the slowly evolving central domain region $a \leq r \leq R(t)$:

$$T(r < R(t), t) = \left(T_{\text{in}} - \frac{P_2^2}{[\ln(R/a) + \varepsilon \ln(b/R)]^2} \right) e^{a-r} + \left(1 - \frac{a^2 P_2^2}{R^2 [\ln(R/a) + \varepsilon \ln(b/R)]^2} \right) e^{\mu^+(r-R)} + \frac{a^2 P_2^2}{r^2 [\ln(R/a) + \varepsilon \ln(b/R)]^2}. \quad (23)$$

The reader can easily follow the same steps and get the solution for the peripheral domain $R(t) \leq r \leq b$. In this case, the resulting composite approximation reads

$$T(r > R(t), t) = \left(T_{\text{out}} - \frac{a^2 P_1^2}{b^2 [\ln(R/a) + \varepsilon \ln(b/R)]^2} \right) e^{r-b} + \left(1 - \frac{a^2 P_1^2}{R^2 [\ln(R/a) + \varepsilon \ln(b/R)]^2} \right) e^{\mu^-(r-R)} + \frac{a^2 P_1^2}{r^2 [\ln(R/a) + \varepsilon \ln(b/R)]^2}. \quad (24)$$

Naturally, in the case of $v = 0$ (that is, $\mu^{\pm} = \pm 1$) and $R = R_*$ we recover our steady-state results (14) and (15).

To complete the solution, we should find $R(t)$. An equation for \dot{R} is obtained from the requirement that the derivative T_r is continuous at $r = R(t)$. Again, only the domain wall terms contribute significantly to the derivative. In this way we obtain

$$\mu^+ \left(1 - \frac{a^2 P_2^2}{R^2 [\ln(R/a) + \varepsilon \ln(b/R)]^2} \right) = \mu^- \left(1 - \frac{a^2 P_1^2}{R^2 [\ln(R/a) + \varepsilon \ln(b/R)]^2} \right). \quad (25)$$

Let us define an auxiliary variable

$$f(R) = - \frac{1 - \frac{a^2 P_1^2}{R^2 [\ln(R/a) + \varepsilon \ln(b/R)]^2}}{1 - \frac{a^2 P_2^2}{R^2 [\ln(R/a) + \varepsilon \ln(b/R)]^2}}. \quad (26)$$

Now, solving Eq. (25) for v , we obtain

$$\dot{R} = v(R) = f^{-1/2} - f^{1/2}. \quad (27)$$

A steady state of Eq. (27) is $v = 0$ or $f(R) = 1$. It is easy to check that this value of f indeed corresponds to the steady-state solution $R = R_*$ of Eq. (16). Notice that Eq. (27) is meaningful only if $0 < f(R) < +\infty$. These conditions can be represented as a double inequality

$$P_2 \varepsilon^{1/2} < \frac{R}{a} \left(\ln \frac{R}{a} + \varepsilon \ln \frac{b}{R} \right) < P_2 \quad (28)$$

that coincides in its form with the criterion (18) of monotonicity of the temperature profile. However, this time it is applied to a time-dependent value of the radius R . One can check that the first-order ordinary differential equation (27) describes relaxation of $R(t)$ towards the fixed point $R = R_*$. In the ‘‘physical’’ space, the domain wall approaches its (pinned) steady-state position. As Eq. (27) is solvable in quadrature for $R(t)$, this completes, in principle, an analytical description of a single domain wall relaxation. Notice that we have not used any close proximity of R to the fixed point R_* . If we want to use it, we can linearize Eq. (27) around $R = R_*$:

$$\frac{d}{dt}(R - R_*) = -\Gamma(R - R_*), \quad (29)$$

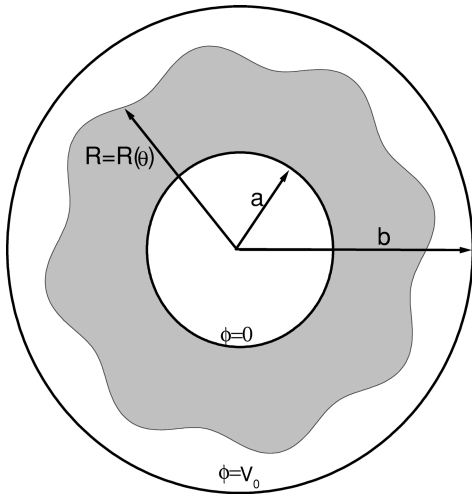


FIG. 4. Annular BR with a small deviation from the azimuthal symmetry.

where

$$\Gamma = \frac{4(1+\varepsilon)[\ln(R_*/a) + \varepsilon \ln(b/R_*) + 1 - \varepsilon]}{(1-\varepsilon)R_*[\ln(R_*/a) + \varepsilon \ln(b/R_*)]}. \quad (30)$$

It is seen that $\Gamma > 0$, so $R = R_*$ is indeed a stable fixed point. Γ is the characteristic relaxation rate of the system. The relaxation time is of order $\Gamma^{-1} = O(L^{-1}) \gg 1$. In physical units, $\Gamma^{-1} \sim Lc/(\kappa A)^{1/2}$, which, in view of our basic assumption $\delta_w/L \ll 1$, is indeed much longer than the cooling (heating) time c/A . This strong inequality justifies our treatment of $R(t)$ and $v(t)$ as slow variables while deriving Eqs. (23) and (24).

Let us return to the double inequality (28). Actually, it is satisfied automatically by the end of the fast first stage of the dynamics, when terms including κ can be neglected. To prove it, one should formally solve Eqs. (7), with all r derivatives neglected, for an arbitrary initial temperature profile and then proceed to the limit of $t \rightarrow \infty$. Finally, in the case of $\varepsilon = 0$ (coexistence of a normal metal and superconductor), the left inequality is always satisfied, while the right one takes the form

$$\frac{R}{a} \ln \frac{R}{a} < P_2. \quad (31)$$

V. AZIMUTHAL STABILITY

Until now we have dealt with the azimuthally symmetric steady state and dynamics of the annular BR. A question arises whether these are stable with respect to small deviations from this symmetry. To answer this question, we consider the same azimuthally symmetric annulus, keep the same boundary conditions for the voltage, but impose a small azimuthal perturbation on the temperature profile. For simplicity, we will limit ourselves to the case of $\varepsilon = 0$ (coexistence of a normal metal and superconductor). Consider a small, time-dependent harmonic perturbation of the azimuthally symmetric domain wall location $R_0(t)$ (see Fig. 4). In polar coordinates $R(\theta, t) = R_0(t)[1 + \delta(t)\cos m\theta]$, where

$\delta(t) \ll 1$ and $m = 1, 2, \dots$ is the azimuthal number of the perturbation.

As before, we start with finding the electric potential from Eq. (1). The potential is zero at $r = a$, while the whole region between the domain wall location $R(\theta, t)$ and external boundary $r = b$ represents an equipotential surface $\phi = V_0$. Therefore, in the step-function approximation (5) for the resistivity, the problem is reduced to solving the Dirichlet problem for Laplace's equation in a slightly deformed annulus. Using the smallness of δ , we are looking for a small θ -dependent correction to the potential that is linear with δ : $\phi(r, \theta) = \phi_0(r) + \delta\phi_1(r, \theta)$, where

$$\phi_0 = \frac{V_0 \ln(r/a)}{\ln(R_0/a)}$$

is the unperturbed potential. Obviously, ϕ_1 must vanish at $r = a$. At the domain wall location we have

$$\phi(r = R(\theta)) = \phi_0(r = R(\theta)) + \delta\phi_1(r = R(\theta)) = V_0. \quad (32)$$

This can be expanded in small δ to yield, in the first order of δ ,

$$\phi_1(r = R_0) \approx -\frac{V_0 \cos m\theta}{\ln(R_0/a)}. \quad (33)$$

The problem is therefore reduced to solving Laplace's equation for ϕ_1 in the circular annulus $a < r < R_0$, but with a θ -dependent boundary condition at $r = R_0$. The solution is

$$\phi_1(r, \theta) = -\frac{V_0(r^m + a^{2m}r^{-m})\cos m\theta}{(R_0^m - a^{2m}R_0^{-m})\ln(R_0/a)}. \quad (34)$$

The next step is to calculate the heating term $(\nabla\phi)^2/\rho$. (We will omit the indices in ρ_2 and P_2 in this section.) We obtain

$$\frac{(\nabla\phi)^2}{\rho} = \frac{(\nabla\phi_0 + \delta\nabla\phi_1)^2}{\rho} = \frac{(\nabla\phi_0)^2 + 2\delta\nabla\phi_0 \cdot \nabla\phi_1 + O(\delta^2)}{\rho}. \quad (35)$$

In polar coordinates, $\nabla\phi_0$ has only a radial component, so only the radial component of $\nabla\phi_1$ survives the dot product. Therefore, keeping only terms linear with respect to δ and writing the result in a scaled form as before, we arrive at

$$\frac{(\nabla\phi)^2}{\rho} = \frac{a^2 P^2}{r^2 \ln^2(R_0/a)^2} \left[1 - 2\delta m \frac{(r^m + a^{2m}r^{-m})\cos m\theta}{R_0^m - a^{2m}R_0^{-m}} \right]. \quad (36)$$

The second term on the right-hand side of Eq. (36) describes a reduction of the Joule heating, as a function of the polar angle, in the regions where the external boundary is more distant. This is understandable, as for the same voltage V_0 a more distant boundary means a larger resistance and hence a smaller electric current and Joule heating. At this stage, we can intuitively predict the resulting temperature dynamics. Let the domain wall slightly protrude outward for some value of the polar angle. As we have just seen, the protrusion zone gets less heat. As a result, the cold peripheral domain of the BR will invade this region, forcing the protrusion to re-

treat. Therefore, we can expect the azimuthally symmetric domain wall dynamics to be stable.

To show it more formally, let us turn to the heat balance equation

$$T_t = T_{rr} + \frac{1}{r}T_r + \frac{1}{r^2}T_{\theta\theta} - T + \frac{(\nabla\phi)^2}{\rho}, \quad r < R(\theta) \quad (37)$$

$$T_t = T_{rr} + \frac{1}{r}T_r + \frac{1}{r^2}T_{\theta\theta} - T, \quad r > R(\theta),$$

with the $(\nabla\phi)^2/\rho$ term from Eq. (36). As before, all the diffusion terms are negligible outside the (weakly curved) domain wall. Inside the domain wall, the curvature terms are negligible, as well as the new term, containing $T_{\theta\theta}$, that includes a large parameter of order L^2 in the denominator [12]. The resulting equation does not include any θ derivatives, so θ (entering the Joule heating term) serves as a parameter only. Therefore, relaxation towards the two-phase steady state proceeds in much the same way as for $m=0$, but this time the domain wall speed and profile are θ dependent. We will limit ourselves to the domain wall dynamics. They can be described by a traveling-wave solution $T(r, \theta, t) = \Theta(r - \int^t v dt')$, where $v = v(\theta, t) = \dot{R}(\theta, t) = \dot{R}_0 + (\dot{R}_0 \delta + R_0 \dot{\delta}) \cos m\theta$. The substitution yields

$$\Theta_{\xi\xi} + v\Theta_{\xi} - \Theta + \frac{[\nabla\phi(r=R_0, \theta)]^2}{\rho} = 0, \quad r < R(\theta) \quad (38)$$

$$\Theta_{\xi\xi} + v\Theta_{\xi} - \Theta = 0, \quad r > R(\theta).$$

Notice that after the substitution of $r=R_0$, the Joule heating term in the first of Eq. (38) becomes r independent, while the θ dependence is preserved. The next steps are identical to those implemented in Sec. III. We find $T_{r>R(\theta)}$ and $T_{r<R(\theta)}$ from Eq. (38), determine the μ^\pm exponents, and require continuity of T_r . Solving the resulting algebraic relation for v , we obtain

$$v = \frac{\frac{(\nabla\phi)^2}{\rho} - 2}{\left[\frac{(\nabla\phi)^2}{\rho} - 1\right]^{1/2}}, \quad (39)$$

with the heating term from Eq. (36), evaluated at $r=R_0$. As we are interested in a small deviation from the azimuthal symmetry, we expand the right-hand side of Eq. (39) in small δ . The zeroth-order term yields Eq. (27) for R_0 , as expected. In first order we obtain after some algebra the equation $\dot{\delta} + \beta\delta = 0$, where

$$\beta = R_0^{-1} \left[\left(\frac{aP}{R_0 \ln(R_0/a)} \right)^2 - 1 \right]^{-3/2} \Phi_m(R_0) \quad (40)$$

and

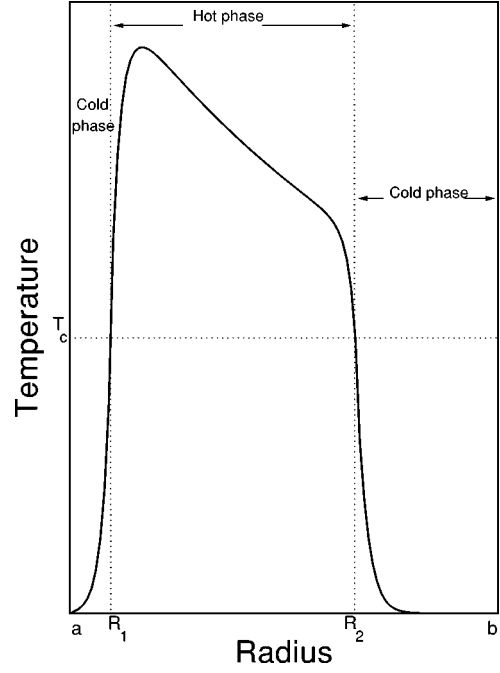


FIG. 5. Annular BR with two concentric domain walls, located at $r=R_1$ and $r=R_2$.

$$\Phi_m(R_0) = \left(1 + m \frac{R_0^m + a^{2m} R_0^{-m}}{R_0^m - a^{2m} R_0^{-m}} \right) \left(\frac{aP}{R_0 \ln(R_0/a)} \right)^4 - 3 \left(\frac{aP}{R_0 \ln(R_0/a)} \right)^2 + 2. \quad (41)$$

A negative β would mean instability, a positive β stability. One can see that $\Phi_m(R_0)$ is a quadratic function of the argument $\{aP/[R_0 \ln(R_0/a)]\}^2$ and this function is always positive. Therefore, $\beta > 0$ and azimuthal symmetry is restored after a small perturbation.

VI. TWO-INTERFACE DYNAMICS AND COARSENING

A ‘‘natural’’ state of the wire BR observed in experiment is that with a hot domain sandwiched between two cold domains [1–3]. The presence of two domain walls in the wire BR lasts for an exponentially long time with respect to L/δ_w . A question arises whether two domain walls can coexist in an annular BR. We will show in this section that the answer to this question is negative.

Consider an azimuthally symmetric initial temperature profile with two domain walls, concentric with the annulus (see Fig. 5). The domain walls’ locations are denoted by R_1 and R_2 , where $R_1 < R_2$. The hot phase zone now lies between two cold phases. The domain walls can move inward or outward in the annulus, each with its own speed. As a result, the hot zone can expand, shrink, or move as a whole. For simplicity, we will assume that the cold phase is superconducting ($\rho_1=0$ and hence $\varepsilon=0$ and $P_1=0$). The Joule heating takes place only in the hot zone and each of the two cold zones has a trivial (zero-temperature) large-scale behavior.

The heating term (4) takes the form

$$\frac{(\nabla\phi)^2}{\rho} = \begin{cases} \frac{a^2 P_2^2}{r^2 \ln(R_2/R_1)^2}, & R_1(t) < r < R_2(t) \\ 0 & \text{otherwise.} \end{cases} \quad (42)$$

The (slowly varying) domain wall speeds are given by $v_1 = \dot{R}_1$ and $v_2 = \dot{R}_2$. Accordingly, there are two ξ variables in the traveling-wave solutions. To get the full solution of the problem, one needs to solve three simple linear equations for the temperature, for each of the three zones, and implement separate matched asymptotics expansion procedures for each of the domain walls and for the two boundary layers. We will limit ourselves to finding the domain walls' speeds. This time one has two pairs of μ exponents, one pair for each of the domain walls:

$$\mu_1^\pm = \frac{-v_1 \pm \sqrt{v_1^2 + 4}}{2}, \quad \mu_2^\pm = \frac{-v_2 \pm \sqrt{v_2^2 + 4}}{2}.$$

In the region of the first domain wall the temperature profile is

$$T_{r \geq R_1} = \left[1 - \frac{a^2 P^2}{R_1^2 \ln(R_2/R_1)^2} \right] e^{\mu_1^- [r - R_1(t)]} + \frac{a^2 P^2}{R_1^2 \ln(R_2/R_1)^2}, \quad (43)$$

$$T_{r \leq R_1} = e^{\mu_1^+ [r - R_1(t)]}.$$

For the second domain wall

$$T_{r \geq R_2} = \left[1 - \frac{a^2 P^2}{R_2^2 \ln(R_2/R_1)^2} \right] e^{\mu_2^- [r - R_2(t)]} + \frac{a^2 P^2}{R_2^2 \ln(R_2/R_1)^2}, \quad (44)$$

$$T_{r \leq R_2} = e^{\mu_2^+ [r - R_2(t)]}.$$

Now we use the continuity of T_r for each of the two domain walls and obtain two algebraic relations. After some algebra, we arrive at two coupled equations

$$\frac{dR_1'}{d\tau} = - \frac{1 - R_1'^2 \ln^2(R_2'/R_1')}{R_1' \ln(R_2'/R_1') [2 - R_1'^2 \ln^2(R_2'/R_1')]^{1/2}}, \quad (45a)$$

$$\frac{dR_2'}{d\tau} = \frac{1 - R_2'^2 \ln^2(R_2'/R_1')}{R_2' \ln(R_2'/R_1') [2 - R_2'^2 \ln^2(R_2'/R_1')]^{1/2}}, \quad (45b)$$

where we have introduced new scaled radii $R_i' = R_i/aP\sqrt{2}$, $i=1$ and 2 , and time $\tau = \sqrt{2}t/aP$. Also, we have denoted $P_2 = P$.

Equations (45) describe interaction between two domain walls. The interaction is relatively strong, as its characteristic time is of the same order as the one-wall relaxation time Γ^{-1} . This time is proportional to L/δ_w , in contrast to the wire BR where the corresponding interaction time is exponentially long with respect to this parameter.

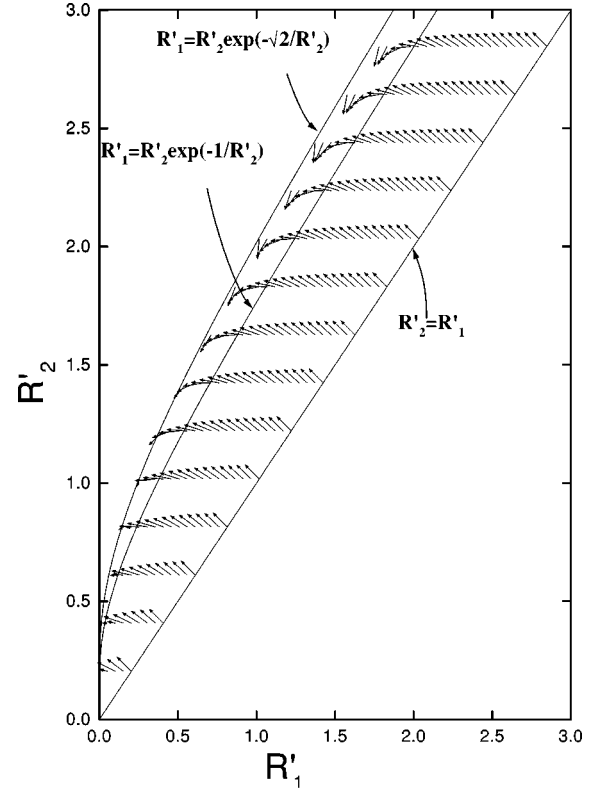


FIG. 6. Phase portrait of the dynamical system (45).

The scaled dynamical system (45) does not include any parameters. It can be conveniently investigated on the phase plane (R'_1, R'_2) (see Fig. 6). Since $R'_2 > R'_1$, we are only interested in the 45° – 90° sector of the first quadrant. Because of symmetry of Eqs. (45), the phase trajectories cross the straight line $R'_2 = R'_1$ at a right angle. Next, not the whole 45° – 90° sector is legitimate, since the expression under the square root in the denominator of Eq. (45b) must be positive. This implies that the relevant part of the phase plane is bounded from above by the line $R'_1 = R'_2 \exp(-\sqrt{2}/R'_2)$, along which all “arrows” point vertically down. Another important line is that for which $\dot{R}'_2 = 0$, that is, $R'_1 = R'_2 \exp(-1/R'_2)$, and the arrows point horizontally to the left along this line. The resulting phase portrait is shown in Fig. 6. After an initial period of time (during which R'_2 may temporarily increase with time), all generic phase points approach a universal trajectory, on which R'_1 and R'_2 both decrease with time. In the physical space it corresponds to motion of the hot domain as a whole inward along a universal path. It is clear from this analysis that no steady state with two domain walls is possible. The first domain wall (characterized by R_1) enters the inner boundary layer first. Of course, the equation for R_1 ceases to be valid when the difference $R_1 - a$ approaches δ_w . At that time one should switch to Eq. (27) for the single-wall dynamics.

Overall, we can interpret the results of this section as universal coarsening in the annular BR. Indeed, for most initial conditions, the coarsening proceeds along a universal path in the phase plane. Finally, only the second domain wall survives, while the first one is “absorbed” by the inner boundary layer and disappears. This coarsening process was verified by numerical simulations with the full thermal balance equation (see the next section).

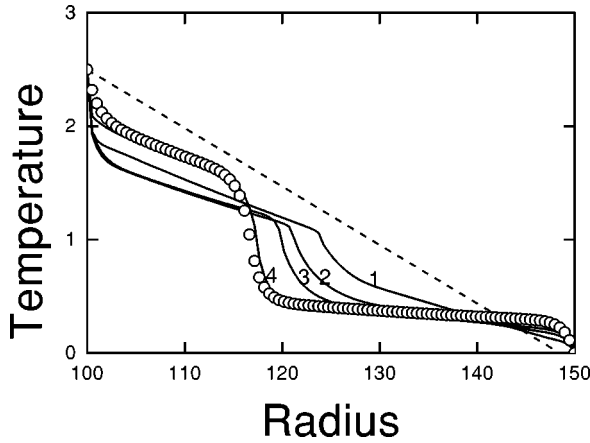


FIG. 7. Numerical simulations of a single domain wall formation and dynamics in the annular BR. Shown are the normalized temperature profiles of the BR versus time. The dashed line represents the initial profile, while the solid lines correspond to $t=0.75$ (profile 1), 1.5 (2), 2.25 (3), and 18.75 (4). Time is measured in normalized units. The theoretical steady-state profile is shown by circles. The parameters are $P_2=0.33$ and $\varepsilon=0.3$.

VII. NUMERICAL SIMULATIONS

The aim of numerical simulations was to verify the predictions of the asymptotic theory of the annular BR that was presented in the previous sections. The first set of simulations included a single domain wall. Here we worked with a scaled thermal balance equation (7) in each of the two regions and employed an implicit scheme of finite differences. At each time step we found R [from the condition $T(R,t)=1$], and then calculated the heating terms for each of the regions $T<1$ and $T>1$. Then we propagated the temperature profiles in each of the regions, updated the value of R , and so on. The process continued until a steady state was reached. In the simulations with two domain walls (the second set of simulations) we employed a similar equation with three separate regions. Here we found R_1 and R_2 , calculated the heating terms in each of the three regions, propagated the solution, updated the values of R_1 and R_2 , and so on. Fixed-temperature boundary conditions were used in all simulations.

As all lengths in the problem were scaled by δ_w , we chose the inner and outer radii a and b of order 10^2 (to satisfy the inequality $L/\delta_w \gg 1$). The number of divisions N was also of order 10^2 , with typical values 100, 150, and 200. In most simulations an increase of N from 150 to 200 did not result in a noticeable increase of accuracy. We used different values of the parameter ε . The value of the heating parameter P_2 was chosen to comply with the double inequality (17) so as to allow the steady-state domain wall to reside on the interval (a,b) .

In the first set of simulations we started with a linear temperature profile and, after a short transient, compared the numerically found domain wall position as a function of time $R(t)$ and the overall temperature profile with those predicted by our theory. Special emphasis was put on checking the steady-state position of the domain wall R_* . Typical simulation results are shown in Fig. 7, where the initial temperature profile (dashed line) and profiles at subsequent times (solid lines) are shown. After a transient, a characteristic

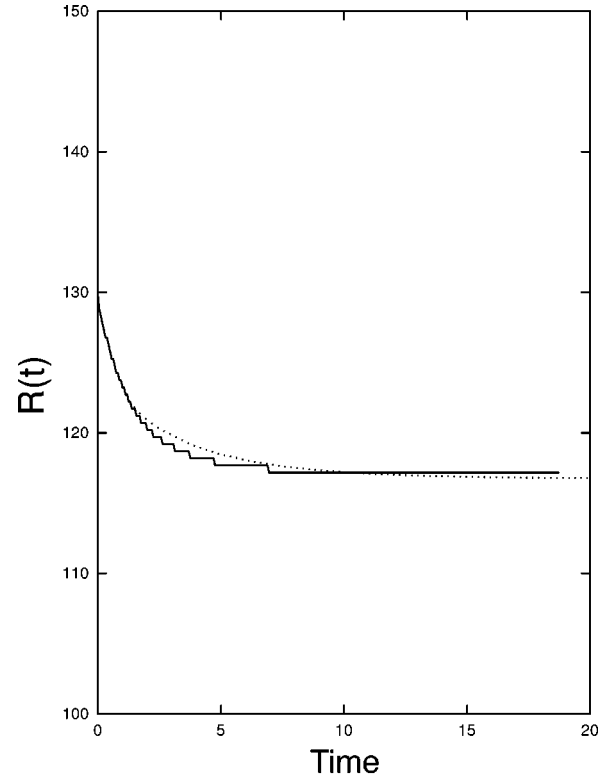


FIG. 8. Same as in Fig. 7, but shown are the dynamics of the domain wall position found numerically (solid line) and predicted by theory (dotted line).

large-scale temperature profile develops, while the domain wall acquires the shape predicted by the theory. It is seen that at long times the temperature profile approaches the theoretical steady-state profile described by Eqs. (14) and (15) with R_* from Eq. (16) (this profile is indicated by circles). Figure 8 shows the domain wall position $R(t)$ as found in the simulations (solid line) and by solving Eq. (27) (dotted line). The results agree within 1% (we used $N=100$ in this example).

The second set of simulations dealt with the dynamics of two domain walls. Results of one simulation are shown in Fig. 9. The initial temperature profile is shown by the dashed line, the profiles at subsequent times by solid lines. Similar to the one-wall case, the large-scale profile develops rapidly. Correspondingly, two pronounced domain walls appear. The walls are moving to the left (inward). Finally, the ‘‘left’’ domain wall (the one with R_1) is absorbed by the inner boundary layer and disappears as predicted. A more quantitative comparison with the theory includes the dynamics of the domain wall radii $R_1(t)$ and $R_2(t)$ as seen in the phase plane (R_2, R_1) . Figure 10 shows R_2 as a function of R_1 as found in the simulations (solid line) and predicted by the dynamical system (45) with the proper initial conditions (dashed line). The comparison shows a good agreement. Also, we checked that different initial conditions with two domain walls approach during coarsening the same ‘‘universal’’ path in the phase plane (R_1, R_2) .

VIII. SUMMARY

We have studied an annular ballast resistor: a simple but nontrivial physical system that shows bistability and pattern

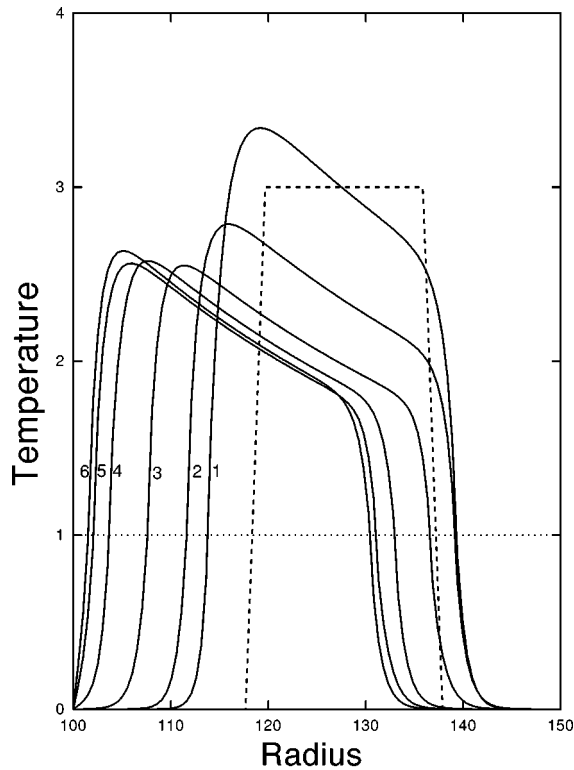


FIG. 9. Numerical simulations of two domain walls' formation and dynamics. Shown are the normalized temperature profiles of the BR versus time. The dashed line represents the initial profile, while the solid lines correspond to $t = 14.06$ (profile 1), 18.75 (2), 42.2 (3), 45.6 (4), 75.0 (5), and 103.1 (6). The parameters are $P_2 = 0.43$ and $\varepsilon = 0$.

formation. The nonuniformity of the electric current density in the annular BR breaks translational symmetry of the temperature domains. This leads to a number of important effects. First, the steady-state position of the domain wall is pinned, that is, uniquely determined by the parameters of the system. Second, this steady state is nonlinearly stable with respect to radial displacements and a domain wall approaches it as a traveling wave with a slowly varying speed. In addition, the steady state is linearly stable with respect to azimuthal perturbations. Third, the annular BR exhibits coarsening. Two domain walls cannot be in equilibrium and the domain wall that is closer to the inner radius of the an-

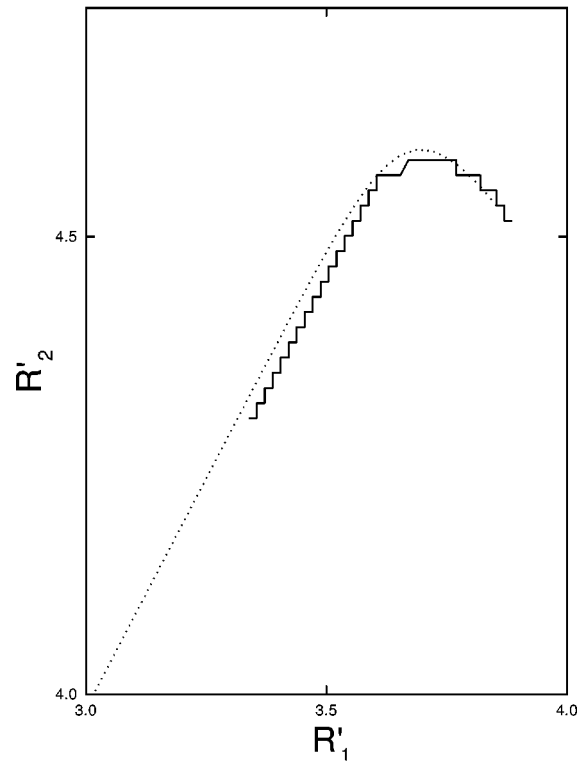


FIG. 10. Same as in Fig. 9, but shown are the dynamics in the phase plane (R'_1, R'_2) of the domain wall positions found numerically (solid line) and predicted by theory (dotted line).

nulus is absorbed by the inner boundary layer and disappears. The coarsening dynamics proceeds along a universal path in the phase plane (R'_1, R'_2) , where R'_1 and R'_2 are the (scaled) domain walls' radii.

Our choice of a simple, steplike function for the temperature dependence of the resistivity has enabled us to study all these effects analytically. The main results of the theory were verified by numerical simulations. It would be interesting to study these effects in experiment.

ACKNOWLEDGMENT

This work was supported in part by a grant from Israel Science Foundation, administered by the Israel Academy of Sciences and Humanities.

-
- [1] V.V. Barelko, V.M. Beibutyan, Yu.E. Volodin, and Ya.B. Zel'dovich, Dokl. Akad. Nauk SSSR **257**, 339 (1981) [Sov. Phys. Dokl. **26**, 335 (1981)].
- [2] A.V. Gurevich and R.G. Mints, Rev. Mod. Phys. **59**, 941 (1987).
- [3] N. Bujanós, J. Pearson, W.D. McCormick, and W. Horsthemke, Phys. Lett. A **127**, 138 (1988).
- [4] F.-J. Elmer, Phys. Rev. A **41**, 4174 (1990).
- [5] A.S. Mikhailov, *Foundations of Synergetics I. Distributed Active Systems* (Springer-Verlag, Berlin, 1990).
- [6] L. Lobban, G. Philippou, and D. Luss, J. Phys. Chem. **93**, 733 (1989).
- [7] B. Meerson and P.V. Sasorov, Phys. Rev. E **53**, 3491 (1996).
- [8] L. Schimansky-Geier, Ch. Züllicke, and E. Schöll, Z. Phys. B **84**, 433 (1991).
- [9] J. Rubinstein and P. Sternberg, IMA J. Appl. Math. **48**, 249 (1992).
- [10] B. Meerson and I. Mitkov, Phys. Rev. E **54**, 4644 (1996).
- [11] E.J. Hinch, *Perturbation Methods* (Cambridge University Press, Cambridge, 1991).
- [12] One can check that this new term gives an additional contribution to damping of the azimuthal perturbations.